

Higher-order modulations of fs laser pulses for GHz frequency domain photon migration system

Huang-Yi Lin,¹ Nanyu Cheng,² Sheng-Hao Tseng,^{2,3} and Ming-Che Chan^{1,*}

¹*Institute of Imaging and Biomedical Photonics, College of Photonics, National Chiao-Tung University, Taiwan*

²*Department of Photonics, National Cheng-Kung University, Taiwan*

³*Advanced Optoelectronic Technology Center, National Cheng-Kung University, Tainan 701, Taiwan*

*mcchan@nctu.edu.tw

Abstract: Except the fundamental modulation frequency, by higher-order-harmonic modulations of mode-locked laser pulses and a simple frequency-demodulation circuit, a novel approach to GHz frequency-domain-photon-migration (FDPM) system was reported. With this novel approach, a wide-band modulation frequency comb is available without any external modulation devices and the only electronics to extract the optical attenuation and phase properties at a selected modulation frequency in FDPM systems are good mixers and lock-in devices. This approach greatly expands the frequency range that could be achieved by conventional FDPM systems and suggests that our system could extract much more information from biological tissues than the conventional FDPM systems. Moreover, this demonstration will be beneficial for discerning the minute change of tissue properties.

©2014 Optical Society of America

OCIS codes: (140.4050) Mode-locked lasers; (170.5280) Photon migration; (290.1990) Diffusion.

References and links

1. A. Cerussi, D. Hsiang, N. Shah, R. Mehta, A. Durkin, J. Butler, and B. J. Tromberg, "Predicting response to breast cancer neoadjuvant chemotherapy using diffuse optical spectroscopy," *Proc. Natl. Acad. Sci. U.S.A.* **104**(10), 4014–4019 (2007).
2. M. Dehaes, P. E. Grant, D. D. Sliva, N. Roche-Labarbe, R. Pienaar, D. A. Boas, M. A. Franceschini, and J. Selb, "Assessment of the frequency-domain multi-distance method to evaluate the brain optical properties: Monte Carlo simulations from neonate to adult," *Biomed. Opt. Express* **2**(3), 552–567 (2011).
3. S. H. Tseng, A. J. Durkin, P. Wilder-Smith, D. Cuccia, F. Bevilacqua, A. G. Durkin, and B. J. Tromberg, "Diffuse, Near Infrared Spectroscopy of in-vivo Oral Tissues," poster in Engineering Foundation Conference. 2003. Banff, Canada.
4. S. H. Tseng, C. K. Hsu, J. Yu-Yun Lee, S. Y. Tzeng, W. R. Chen, and Y. K. Liaw, "Noninvasive evaluation of collagen and hemoglobin contents and scattering property of in vivo keloid scars and normal skin using diffuse reflectance spectroscopy: pilot study," *J. Biomed. Opt.* **17**(7), 077051 (2012).
5. C. D'Andrea, A. Nevin, A. Farina, A. Bassi, and R. Cubeddu, "Assessment of variations in moisture content of wood using time-resolved diffuse optical spectroscopy," *Appl. Opt.* **48**(4), B87–B93 (2009).
6. J. Johansson, S. Folestad, M. Josefson, A. Sparén, C. Abrahamsson, S. Andersson-Engels, S. Svanberg, and A. Sparen, "Time-Resolved NIR/Vis Spectroscopy for Analysis of Solids: Pharmaceutical Tablets," *Appl. Spectrosc.* **56**(6), 725–731 (2002).
7. A. Bassi, A. Farina, C. D'Andrea, A. Pifferi, G. Valentini, and R. Cubeddu, "Portable, large-bandwidth time-resolved system for diffuse optical spectroscopy," *Opt. Express* **15**(22), 14482–14487 (2007).
8. T. H. Pham, O. Coquoz, J. B. Fishkin, E. Anderson, and B. J. Tromberg, "Broad bandwidth frequency domain instrument for quantitative tissue optical spectroscopy," *Rev. Sci. Instrum.* **71**(6), 2500–2513 (2000).
9. S. H. Tseng, P. Bargo, A. Durkin, and N. Kollias, "Chromophore concentrations, absorption and scattering properties of human skin in-vivo," *Opt. Express* **17**(17), 14599–14617 (2009).
10. J. B. Fishkin, P. T. C. So, A. E. Cerussi, S. Fantini, M. A. Franceschini, and E. Gratton, "Frequency-Domain Method for Measuring Spectral Properties in Multiple-Scattering Media: Methemoglobin Absorption Spectrum in a Tissue-like Phantom," *Appl. Opt.* **34**(7), 1143–1155 (1995).
11. F. Bevilacqua, J. S. You, C. K. Hayakawa, and V. Venugopalan, "Sampling tissue volumes using frequency-domain photon migration," *Phys. Rev. E Stat. Nonlin. Soft Matter Phys.* **69**(5), 051908 (2004).
12. B. J. Tromberg, L. O. Svaasand, T. T. Tsay, and R. C. Haskell, "Properties of photon density waves in multiple-scattering media," *Appl. Opt.* **32**(4), 607–616 (1993).
13. J. Wang, S. D. Jiang, K. D. Paulsen, and B. W. Pogue, "Broadband frequency-domain near-infrared spectral tomography using a mode-locked Ti:sapphire laser," *Appl. Opt.* **48**(10), D198–D207 (2009).

14. Y. Bai, D. M. Ren, W. J. Zhao, Y. C. Qu, L. M. Qian, and Z. L. Chen, "Heterodyne Doppler velocity measurement of moving targets by mode-locked pulse laser," *Opt. Express* **20**(2), 764–768 (2012).
15. J. T. Verdeyener, *Laser Electronics* (Prentice-Hall, 1995).
16. J. W. Shi, F. M. Kuo, and J. E. Bowers, "Design and Analysis of Ultra-High-Speed Near-Ballistic Uni-Traveling-Carrier Photodiodes Under a 50-Omega Load for High-Power Performance," *IEEE Photon. Technol. Lett.* **24**(7), 533–535 (2012).
17. S. Haykin, *Communication Systems* (John Wiley, 1994).
18. S. A. Prahl, M. J. van Gemert, and A. J. Welch, "Determining the optical properties of turbid mediaby using the adding-doubling method," *Appl. Opt.* **32**(4), 559–568 (1993).
19. L. H. Wang, S. L. Jacques, and L. Q. Zheng, "Mcml - Monte-Carlo Modeling of Light Transport in Multilayered Tissues," *Comput. Meth. Prog. Biol.* **47**(2), 131–146 (1995).
20. R. C. Haskell, L. O. Svaasand, T. T. Tsay, T. C. Feng, M. S. McAdams, and B. J. Tromberg, "Boundary Conditions for the Diffusion Equation in Radiative Transfer," *J. Opt. Soc. Am. A* **11**(10), 2727–2741 (1994).
21. D. A. Boas, M. A. O'Leary, B. Chance, and A. G. Yodh, "Detection and characterization of optical inhomogeneities with diffuse photon density waves: a signal-to-noise analysis," *Appl. Opt.* **36**(1), 75–92 (1997).

1. Introduction

Diffuse Optical Spectroscopy (DOS) has been applied to study the properties of various biological tissues. DOS is a model based technique and can be used to noninvasively determine the average absorption and scattering coefficients and chromophore concentrations of deep or superficial tissues, such as breast, brain, and skin [1–4] and non-biological samples [5, 6]. The derived information can further be utilized for monitoring the condition of tissues and/or performing diagnosis or prognosis [1, 4]. Several types of light source can be employed in the DOS setup, such as pulsed, intensity modulated light sources, and continuous wave [7–9]. These light sources have to work in conjunction with proper light detecting schemes. For example, a pulsed light source usually works with a time correlated single photon counting system to obtain the time point spread function of turbid samples [7]. On the other hand, a high speed detector is generally used to detect the diffused photons generated from an intensity modulated light, and the detected signal would be further processed to determine the amplitude demodulation and phase delay introduced by samples [8]. By measuring the response of the samples with respect to a certain light source and fit the data to an appropriate photon transport model, the optical properties of samples can be derived.

DOS systems that employ intensity modulated light sources are usually termed as the Frequency Domain Photon Migration (FDPM) technique [1]. In a typical FDPM system, laser diodes are modulated with radio frequency (RF) signals to generate intensity modulated light in the range from a few MHz to 1 GHz with a modulation depth as close to unity as possible. Single-modulation-frequency and multiple-modulation-frequency FDPM systems have both been successfully applied to study turbid samples [8, 10]. It has been reported that at higher modulation frequencies, the phase shift introduced by the variation of optical properties is larger [11, 12]. Such phenomenon is beneficial for discerning the minute change of tissue properties and thus is helpful for prognosis and biological status monitoring. In addition, because the light intensity is strongly attenuated in most biological tissues due to absorption and scattering, to acquire proper frequency domain diffuse reflectance, it is important to drive the laser at a modulation depth as close to one as possible. Up until now, the upper bound of laser modulation frequencies of most FDPM systems has been limited below around 1.0 GHz [8] and the modulation depth generally rolls off quickly with the modulation frequency. This limitation comes from the intrinsic nature of laser diodes; most of them are not designed to operate at high modulation frequencies with a close-to-unity modulation depth.

Alternatively, mode-locked lasers, generating pico-second or even femtosecond pulses, with proper light detection scheme can also be used as the light source of FDPM systems. Previous studies [13, 14] have shown that mode-locked laser pulses have higher modulation depth and greater power levels compared with externally modulated laser diodes usually utilized in FDPM system. Such great power levels and high modulation depths of mode-locked laser pulses are extremely helpful for increasing the signal-to-noise ratio of FDPM systems working at large source-detector separations for studying the optical properties of thick tissues. Based mode-locked Ti:Sapphire laser pulses, by using the fundamental intrinsic modulation frequency which is equal to the laser repetition rate, Wang and his collaborators

have demonstrated FDPDM at the 80MHz fundamental intrinsic modulation frequency in the 690-850 nm wavelength regime to study the tissue hemoglobin and oxygen saturation [13].

Both the direct modulation method of laser diodes [8] and the fundamental modulations of mode-locked laser pulses [13, 14] have not shown the capability to work at modulation frequencies beyond 1.0 GHz. Nevertheless, to further increase the sensitivity of FDPDM systems to a slight change of tissue properties, it is essential to extend the light source modulation frequency beyond 1.0 GHz.

In this paper, based on higher-order-harmonic modulations of excitation mode-locked laser pulses and a frequency demodulation circuit, we report a novel GHz FDPDM system providing multiple modulation frequencies within a broadband bandwidth without any external modulation devices. In the frequency demodulation circuit, the only electronics to extract the optical attenuation and phase properties at a selected modulation frequency are good mixers and lock-in devices. Finally, corresponding optical attenuation and scattering properties at different modulation frequencies inside samples can be sequentially retrieved. Without any external modulators in the source side, the demonstrated high-frequency-modulated FDPDM system, which breaks the frequency limitation of modulated optical source, shows great potential for future high-sensitive FDPDM detections. Moreover, mode-locked laser pulses are with better modulation depth than other internally or externally modulated light source which offers the benefits to increase the signal to noise ratio. It is also advantageous to employ a pulse laser in the clinical FDPDM system because low average power is required, which reduces tissue damage effect.

2. Higher-order modulations inside mode-locked laser pulses

Figure 1 illustrates the operation principle of this work. In the time domain, mode-locked laser pulses, as shown in Fig. 1(a), are intrinsically repetitive unity optical modulations with periods T and durations $\Delta\tau$. As shown in Fig. 1(b), the Fourier transform of mode-locked pulse trains is a periodic modulation in the frequency domain with a period $1/T$, which implies mode-locked laser pulses are capable of offering a series of modulation frequencies simultaneously. The modulation frequency bandwidth, $(\Delta\nu)$, is inversely proportional to the pulse width $(\Delta\tau)$, as shown in Fig. 1(c). In previous studies [13, 14], the application of mode-locked laser on FDPDM systems was limited in the fundamental modulations of laser pulses, which is equal to $(1/T)$ as shown in Fig. 1(b). Inside the mode-locked laser pulses, the higher-order modulations, ranging from $(2/T)$ to $(\Delta\nu)$, have the capability to provide modulation frequencies beyond tens of GHz depending on the pulse width.

For a transform-limited Gaussian femtosecond pulses, the time-bandwidth product of $(\Delta\tau)$ and $(\Delta\nu)$ must be greater than 0.441 [15]. Typically, a 100-fs transform-limited mode-locked laser pulses provides a 4.41 THz maximum modulation bandwidth, which is one order greater than the detectable bandwidth of existing photo-detector and detection electronics [16]. Compared with other light sources in FDPDM whose modulation bandwidth is limited by light source or external modulators, femtosecond lasers offer ultra-broadband modulation frequencies and the intrinsic unity modulation depth, which are promising tool for discerning the minute change of tissue properties.

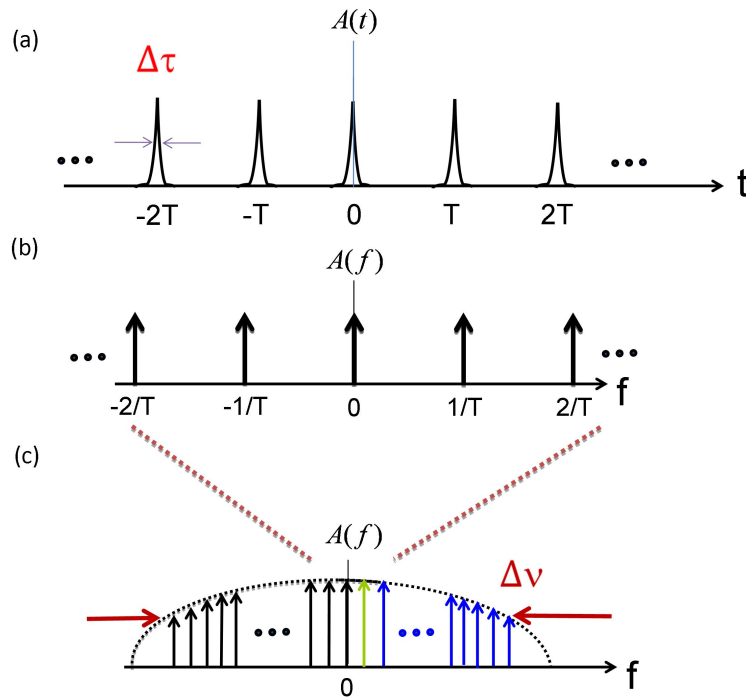


Fig. 1. Operation principles of high-frequency FDPM system. (a): Periodic mode-locked laser pulse trains with period T and pulse duration $\Delta\tau$. (b): The Fourier transform of mode-locked laser pulse trains. $A(f)$ means the amplitude in the frequency domain and is equal to the Fourier transform of $A(t)$. (c): The bandwidth Fourier transforms in the frequency domain is determined by the pulse width. The fundamental modulation frequency (demonstrated in previous report) is labeled by a green line and the higher-order modulation frequencies (demonstrated in this report) are labeled by blue lines.

3. Experimental setup

The experimental setup is shown in Fig. 2. The excitation laser was a compact mode-locked Ytterbium-YAG laser with a 54.79 MHz fundamental repetition rate, which is equal to the spacing between nearby modulation frequencies. In the setup, mode-locked laser pulses provide a wide-band modulation frequency comb is available without any external modulation devices. The full-width-half-maximum of laser spectrum was 7.89 nm with a 1022.5 nm central wavelength. The measured pulse duration was 252.6 fs. Part of the laser output was detected by a photo-detector (PD1) as a reference. Another part of light source output, delivered by a multi-mode fiber with a 400 μm core diameter, illuminated on the sample. Diffusely reflected photons were collected from a sample with a series of modulation frequencies and guided to another avalanche detector (PD2) by another multi-mode fiber. The output of PD1 and PD2 are connected to a home-build frequency demodulation circuit, which is similar to the coherent detection scheme in the communication circuits [17] and the only electronics needed to have higher harmonics are good mixers and lock-in amplifiers in our design.

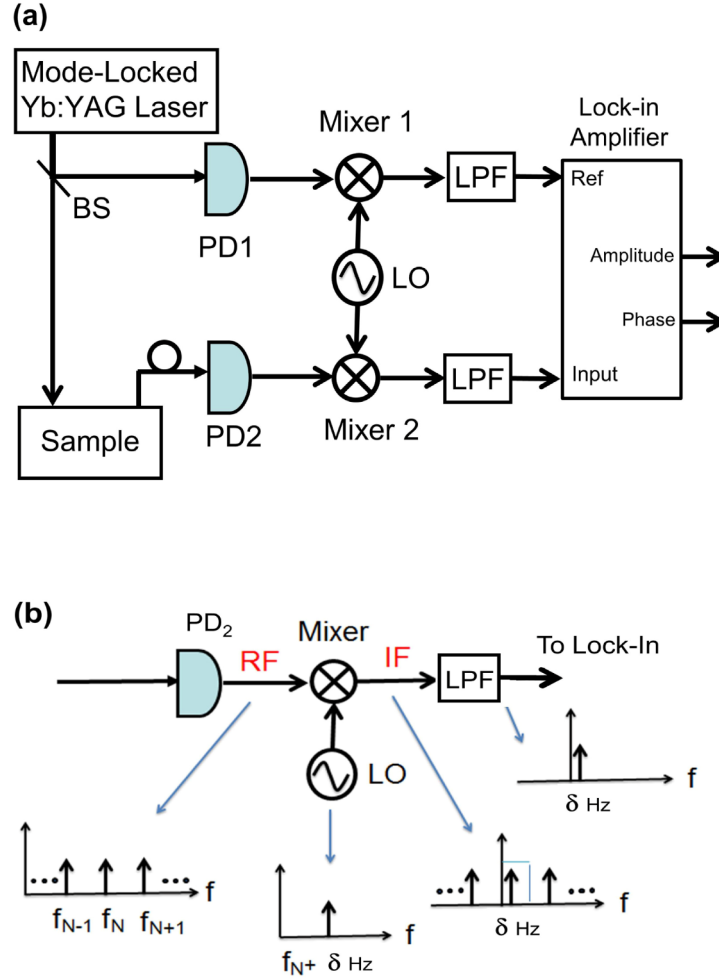


Fig. 2. (a) Schematic for proposed FDPM system. Abbreviations: BS beam splitter, PD1 and PD2 photodetector, LPF 10MHz electrical low-pass filters. (b) Operation principles of frequency demodulation circuits. δ is the detuning frequency for lock-in detection.

The working principle of frequency demodulation circuit is shown in Fig. 2(b). At the output of PD2, the reflected radio frequency (RF) signals from the sample, RF, are composed with a series of modulation frequencies and can be expressed as:

$$RF = \sum_k A_k \cos(2\pi f_k t + \Phi_k) \quad (1)$$

where A_k and Φ_k are the amplitude and phase of diffused photons from the sample with a modulation frequency, f_k .

To measure the amplitude and phase of A_N and Φ_N at modulation frequency f_N , the output signal from the local oscillator (LO), should be in the form as:

$$LO = A_c \cos(2\pi f_c t + \Phi_c) \quad (2)$$

where $f_c = f_N + \delta$, is the frequency of LO and A_c is the amplitude of LO. δ is the reference frequency for lock-in detection, equal to 100 kHz in this experiment. Φ_c is the phase shift induced by the LO.

The input of mixers with modulation frequency, f_N , can be expressed as:

$$RF = A_N \cos(2\pi f_N t + \Phi_N) \quad (3)$$

where A_N and Φ_N is the amplitude and phase of diffused photons from the sample with a modulation frequency f_N . The output from the mixer, the intermediate frequency (IF), is proportional to the product of RF and LO, and can be expressed as:

$$IF = \left(\frac{1}{2}\right) A_N A_c \cos[2\pi(2f_N t + \delta)t + (\Phi_N + \Phi_c)] + \left(\frac{1}{2}\right) A_N A_c \cos[2\pi(\delta)t + (\Phi_N - \Phi_c)] \quad (4)$$

The first term in Eq. (4) represented an up-converted signals with a carrier frequency $2f_N t + \delta$, whereas the second term is proportional to A_N with a carrier frequency δ from the sample. The second term can be filtered out by a low pass filter as shown in Fig. 2(b). In the reference arm, the signal of PD1 with modulation frequency, f_N , has a similar form in Eq. (4). Then, two filtered reference and signal outputs were connected to a lock-in amplifier (SR830, Stanford Research Systems) and the contributed amplitude, A_N , and relative phase, Φ_N , of photon density waves from the sample with a modulation frequency, f_N , were measured. By sequentially changing frequencies from local oscillator, we can get changes in photon density waves in amplitude and phase as a function of modulation frequency. Then, the corresponding macroscopic absorption and scattering coefficients were calculated.

4. Results and discussion

The bandwidth in a FDPM system is both determined by the maximum optical modulation frequency (OMF) that a light source can provide and the maximum electronic detectable frequency (EDF) in a FDPM system. In this experiment, to quantitatively characterize maximum OMF in the demonstrated FDPM systems, we measure the optical spectrum and intensity autocorrelation of laser pulses, as shown in Figs. 3(a) and 3(b). From Fig. 3(a), the full-width-half-maximum of laser spectrum was 7.89 nm with a 1022.5 nm central wavelength. The corresponding full-width-half-maximum bandwidth in frequency is 2.26 THz. The full-width-half-maximum bandwidth of the mode-locked laser pulses sets the upper limit of OMF. In this experiment, the modulation frequency 3dB bandwidth is 2.26 THz, corresponding to 195.1 fs transform-limited pulse duration. However, due to the pulse chirp, the pulse duration is usually not transform-limited so that the practical OMF, determined by the pulsewidth, is smaller than full-width-half-maximum modulation bandwidth. Practical OMF decreases with the pulse-broadening. The measured pulse duration at the sample was 252.6 fs, which implies the practical OMF in our source was 1.75 THz. To increase practical OMF, the laser pulses must be further compressed.

Figure 3(c) shows the RF spectrum of the pulse train, which was measured by a photo-detector (PD2 in Fig. 2(b)) and a RF spectrum analyzer. From Fig. 3(c), we can experimentally show that mode-locked laser pulses can be regarded as the combination of multiple harmonic modulation signals whose frequency spacing between nearby modulations is equal to the laser fundamental repetition rate (54.78 MHz). According to Fig. 3(c), the 3dB bandwidth of EDF was 1.003 GHz, arising from the limitations of the amplified detector (PD2). In the frequency demodulation circuit, shown in Fig. 2(b), the 3dB bandwidth is the bottleneck of the maximum EDF since the bandwidth of frequency mixer and local oscillator are larger than that of amplified detector.

Figure 3(d) shows the relationship between OMF and EDF in previous work and this demonstrated work. As shown in Fig. 3(d), in previous reports [8], the EDF was always larger than maximum OMF that a light source can provide. Thus, the maximum operation frequency in the FDPM was always on the order of 1 GHz. However, in this work, excited by the higher-order modulations of femtosecond pulses, practical OMF was greatly extended to the order of THz, which is much larger than any EDF. The modulation frequency in the FDPM system could be increased up to several hundred of GHz if the speed of electronic system can be further upgraded by high speed detectors, such as metal-semiconductor-metal traveling

wave photo-detectors with a more than 100 GHz bandwidth as shown in the dashed lines of Fig. 3(d) [16].

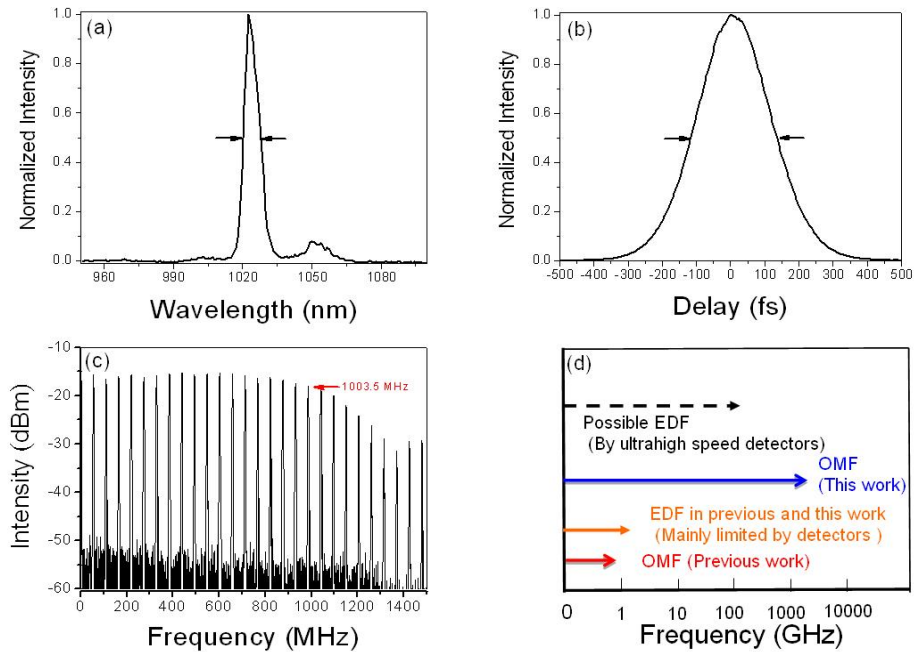


Fig. 3. (a) Optical spectrum and (b) auto-correlation traces of the excitation femtosecond pulses. (c) Electrical spectrum of the modulated signals. (d) The relationship between OMF and EDF in previous work and this work.

Frequency domain diffuse reflectance of a tissue simulating liquid phantom at source-detector separations of 8 and 10 mm were measured. The system response was calibrated by taking the ratio of the amplitudes and the difference of the phases measured at source-detector separations of 8 and 10 mm. The measured amplitude ratio and the phase difference between the two source-detector separations at various frequencies are shown as squares in Fig. 4. The data were then fit to a photon diffusion theory to extract the absorption and the reduced scattering coefficients of the liquid phantom [18]. The photon diffusion theory is usually employed for such purpose for its computational efficiency and adequate accuracy. The best fit of the diffusion theory to the raw data is demonstrated as lines in Fig. 4. The liquid phantom was composed of water, Lipofundin, and Nigrosin. To obtain the benchmark optical properties of the liquid phantom, we filled a 5cm*5cm*2.5mm cuvette with the liquid phantom and measured the total transmission and reflection using an integrating sphere. The measurement results were then fed to an inverse adding-doubling routine to calculate the optical properties of the liquid phantom. The optical properties, including the absorption coefficient μ_a and the reduced scattering coefficient μ_s , of the liquid phantom at 1030nm were both derived from benchmark and the mode-locked based FDP system. Their values were $\mu_a = 0.026/\text{mm}$, $\mu_s = 0.730/\text{mm}$, and $\mu_a = 0.023/\text{mm}$, $\mu_s = 0.618/\text{mm}$, respectively.

The percent deviation of the recovered absorption and the reduced scattering coefficient of our FDP system from the bench mark values are 11.5% and 15.3%, respectively. Compared with a network analyzer based FDP system described by Pham et al [8], which had optical properties recovery errors within 10% and 6% for absorption and reduced scattering coefficients, respectively, the observed difference between network analyzer based FDP system and the demonstrated FDP system leads us to further research on the -improvements when we upgraded the system modulation frequency toward ten Giga-hertz regime.

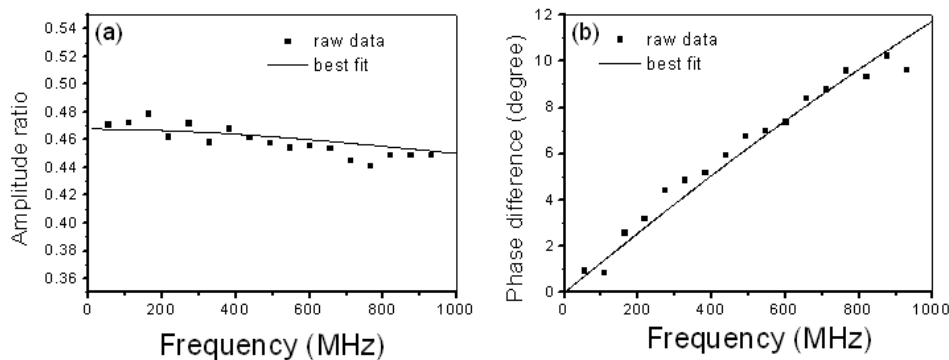


Fig. 4. (a) Amplitude ratio and (b) phase difference as a function of frequency. Squares and lines represent the raw data and the best fit of the diffusion theory, respectively.

In this study, we employed a least squares fitting algorithm “lsqcurvefit” function from Matlab to work in conjunction with the photon diffusion theory to solve the inverse problem. The accuracy of the recovered optical properties strongly relies on the faithfulness of the photon transport model. We found that the amplitude and the phase calculated from the diffusion model deviated from those calculated from the Monte Carlo model, adapted from the one developed by Wang [19], by around 5% and 1 degree, respectively, at modulation frequency of 500 MHz and for optical properties closed to those described above. Thus the deviation of the recovered optical properties from the benchmark values may be reduced by using a more faithful photon transport model, such as Monte Carlo based models. Besides, the deviation could be further reduced by employing electronic components of better specifications to minimize the noise in the system.

It is worth noting that Haskell et al. [20], indicated that in practical terms the standard diffusion theory in frequency domain has an upper limit in the tens of Giga-hertz region. Thus, as the source modulation frequency extending to higher than ten Giga-hertz, it is not suitable to employ a standard diffusion model to describe photon transport and a more rigorous model such as Monte Carlo model should be used instead. Moreover, a high frequency photon wave (ex: 1 THz) is also subject to a high attenuation [21] consequently, the detection responsibility or input source power should be increased to improve the overall signal to noise ratio.

5. Conclusions

In conclusion, we propose a novel FDPM system that does not require direct or indirect laser amplitude modulation. Our system greatly expands the frequency range that could be achieved by conventional FDPM systems from around 1 GHz to tens or hundreds GHz depending on the pulse width of the laser source and the photo detector bandwidth. This broad frequency range suggests that our proposed system could extract much more information from biological tissues than the conventional FDPM systems, and theoretically may retrieve information comparable to that obtained by the time resolved DOS systems. Moreover, the cost of our system would be similar or lower than the conventional FDPM systems and much lower than the time domain counterparts. In addition, it is advantageous to employ a pulse laser in the system because such light source has low average power to avoid tissue damage and has high instantaneous power to increase measurement signal to noise ratio. Although we only demonstrate the phantom measurement at modulation frequencies of up to 1 GHz, the maximal measurable modulation frequency can be readily elevated to 10 GHz by replacing the mixers and photo detectors in our system with better ones. An improved version of our system that covers proper wavelength range for recovering chromophore concentrations of biological tissues is currently being developed and will be applied to in-vivo studies in the near future.

Acknowledgments

The authors acknowledge Dr. Kung-Hsun Lin for loaning the lock-in amplifier and Profs. Sheng-Kwang Hwang, Chien Chou and Chin-Lung Yang for their helpful suggestions. The research is supported in part by the National Science Council of Taiwan, ROC (NSC-100-2221-E-009-092-MY3 and NSC-102-2221-E-006-248-MY2) and the Chi-Mei Medical Research Center in Tainan.